

Lowering the Barrier to C–H Activation at Ir^{III} through Pincer Ligand Design

Sophie B. Rubashkin, Wan-Yi Chu, and Karen I. Goldberg*

Cite This: *Organometallics* 2021, 40, 1296–1302

Read Online

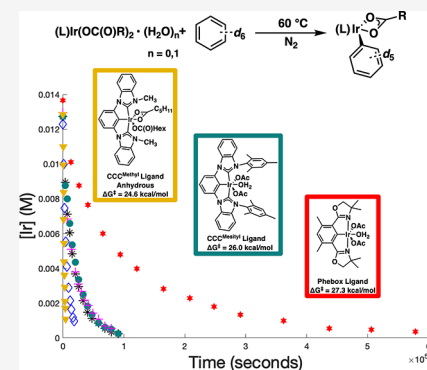
ACCESS |

Metrics & More

Article Recommendations

Supporting Information

ABSTRACT: Selective C–H activation of benzene and *n*-octane under mild conditions by a pincer Ir^{III} carboxylate complex, (CCC^{Mesityl})Ir(OAc)₂(OH₂) (1a), is described. A kinetic study of benzene activation was undertaken, and the resulting Eyring analysis informed the design of a ^tButylCCC^{Methyl}-ligated Ir^{III} carboxylate, which exhibited a ΔG[‡] value for the reaction lower than that observed for 1a. Elimination of the aquo ligand was found to further lower the ΔG[‡] value of benzene activation, enabling C–H activation by Ir^{III} at temperatures as low as 30 °C.



INTRODUCTION

Commercial-scale selective catalytic conversion of alkanes directly to value-added products remains a prominent “holy grail”.^{1,2} Some of the most promising catalysts for such transformations have been thermally robust phosphine (PCP) and phosphinite (POCOP) pincer-ligated Ir compounds, which can catalyze alkane dehydrogenation reactions and are also used as the alkane dehydrogenation catalysts in alkane metathesis.^{3,4} For commercial-scale alkane oxidation, the use of oxygen as the oxidant is desirable from both economic and green chemistry perspectives. However, many organometallic species that can selectively activate C–H bonds are not stable to oxygen. For example, the PCP and POCOP ligated Ir alkane dehydrogenation catalysts cleave alkane C–H bonds via oxidative addition to a low-valent 14-electron Ir^I species, and this highly reactive intermediate is incompatible with O₂ and H₂O.^{5,6} Furthermore, the high temperatures often used for alkane activation are problematic, as alkanes react with O₂ at temperatures above 125 °C to unselectively produce various oxygenates.⁷

The Ir^{III} complex (Phebox)Ir(OAc)₂(OH₂) (Phebox = 2,6-bis(4,4-dimethyloxazolonyl)-3,5-dimethylphenyl) was reported to require temperatures upward of 160 °C to activate *n*-octane and form an Ir^{III}-octyl complex.⁸ In contrast to the PCP- and POCOP-ligated Ir complexes, such C–H bond activations proceed via concerted metalation–deprotonation (CMD) mechanisms, which maintain a high-valent Ir^{III} oxidation state.^{7–11} CMD mechanisms for C–H activation are notable in their ability to operate under aerobic conditions.^{12–14} Further studies demonstrated that (Phebox)Ir(Octyl)(OAc) could undergo β-hydride elimination to form (Phebox)Ir(H)-

(OAc) and olefin and that the Ir–H product reacts with O₂ and HOAc to regenerate the starting (Phebox)Ir(OAc)₂(OH₂) complex at moderate temperatures, establishing a potential cycle for aerobic alkane dehydrogenation.^{9,15–17}

To enable the use of oxygen in alkane functionalization reactions such as alkane dehydrogenation mediated by (Phebox)Ir(OAc)₂(OH₂), the temperature required for the C–H activation step would need to be substantially reduced (<125 °C). Experimental studies determined that changing the identity of the carboxylate ligands did not significantly affect the temperature at which the C–H bond activation occurred.¹⁸ Computational results, however, did suggest that modification of the tridentate pincer ligand could affect the C–H activation barrier.¹⁹ Herein we report that, through using bis-(benzimidazol-2-ylidene)phenyl ligands on Ir, C–H activation is promoted at significantly lower temperatures.

RESULTS AND DISCUSSION

(CCC^{Mesityl})Ir(OAc)₂(OH₂) (1a) was prepared by heating (CCC^{Mesityl})Ir(H)(Cl)(DCM)²⁰ (R^{CCC^{Mesityl}} = bis-(mesitylbenzimidazol-2-ylidene)phenyl) with excess silver acetate in dichloromethane (Scheme 1). The ¹H NMR spectrum of 1a shows a single resonance corresponding to

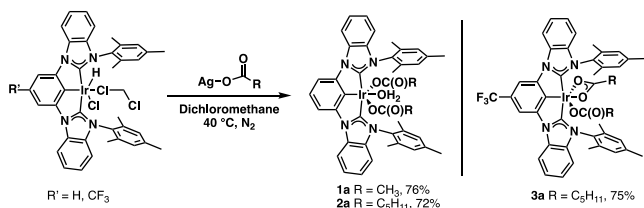
Received: February 9, 2021

Published: April 28, 2021



the two symmetrical acetate ligands along with signals for the hydrogens on the $\text{CCC}^{\text{Mesityl}}$ ligand.

Scheme 1. Synthesis of $(\text{RCCC}^{\text{Mesityl}})\text{Ir}$ Carboxylates



The protons for the aquo ligand were not observed in the ^1H NMR spectrum in dry solvents, but X-ray crystallographic data clearly show the coordination of a water molecule (Figure 1, left).

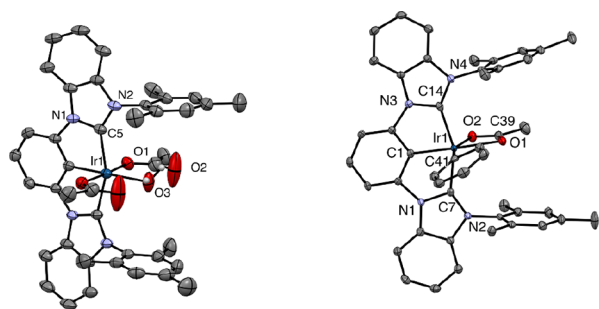
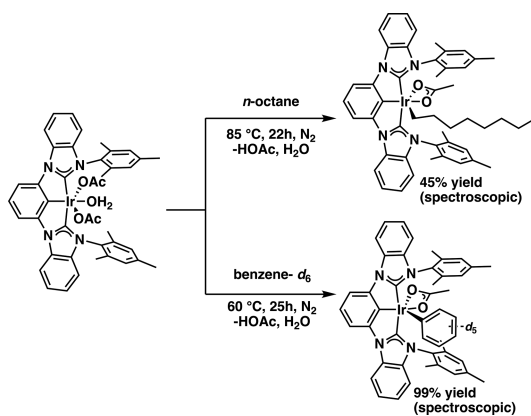


Figure 1. ORTEP diagram of complexes **1a** (left) and **1b** (right) shown with thermal ellipsoids given at the 50% probability level. Hydrogen atoms are omitted for clarity. See the Supporting Information for bond metrics.

Complex **1a** exhibited a significantly higher activity with respect to alkane C–H bond activation in comparison to its Phebox analogue. Nishiyama and co-workers demonstrated that the reaction of $(\text{Phebox})\text{Ir}(\text{OAc})_2(\text{OH}_2)$ with *n*-octane in the presence of K_2CO_3 at 160 °C required over 70 h to generate $(\text{Phebox})\text{Ir}(\text{octyl})(\text{OAc})$ in 78% isolated yield.⁸ Heating complex **1a** in a very dilute (0.11 mM **1a**) solution of neat *n*-octane at 85 °C for 22 h resulted in formation of a new $\text{CCC}^{\text{Mesityl}}$ -containing species in 45% spectroscopic yield (Scheme 2, top). The dilute conditions were necessary due to the very limited solubility of **1a**. Increasing the reaction temperature to 105 °C achieved a 77% spectroscopic yield

Scheme 2. Alkane and Arene Activation by **1a**



after 22 h. Further characterization by $^{13}\text{C}\{^1\text{H}\}$ NMR and mass spectrometry confirmed that this new species is $(\text{CCC}^{\text{Mesityl}})\text{Ir}(\text{Octyl})(\text{OAc})$. Utilization of the CF_3 -substituted CCC-ligand allowed for crystallization of the Ir-octyl species, and the solid-state structure is shown in Figure S10. Notably, no reaction between $(\text{Phebox})\text{Ir}(\text{OAc})_2(\text{OH}_2)$ and *n*-octane was discernible after 24 h at 105 °C.

The very poor solubility of **1a** in neat alkane made it challenging to carry out in-depth solution studies of its reactions. To improve the solubility, an analogue of **1a**, $(\text{CCC}^{\text{Mesityl}})\text{Ir}(\text{OC}(\text{O})\text{Hex})_2(\text{OH}_2)$ (**2a**; Scheme 1), was prepared using silver hexanoate and $(\text{CCC}^{\text{Mesityl}})\text{Ir}(\text{H})(\text{Cl})$ -(DCM).²⁰ The hexanoate ligands allowed for solution studies of C–H activation at a greater concentration in neat *n*-octane at 85 °C (0.52 mM **2a**), but the product mixtures were difficult to separate due to the similar solubilities of **2a** and the presumed $(\text{CCC}^{\text{Mesityl}})\text{Ir}(\text{Octyl})(\text{OC}(\text{O})\text{Hex})$.

To gain insight into why the $\text{CCC}^{\text{Mesityl}}$ complexes were more reactive than the Phebox derivatives in C–H bond activation, the reactions of the Ir compounds were studied in benzene, where solubility was not an issue. Complex **1a** was found to activate C_6D_6 in quantitative yield to form the corresponding complex $(\text{CCC}^{\text{Mesityl}})\text{Ir}(\text{Phenyl-}d_5)(\text{OAc})$ (**1b**) at 100 °C within 1.5 h, under a N₂ or O₂ atmosphere (Scheme 2, bottom). **1b** was fully characterized, including by X-ray crystallography (Figure 1, right), and is air- and moisture-stable both in solution and in the solid state. At 60 °C, the reaction of **1a** with C_6D_6 reached 99% conversion to **1b** after 25 h, while thermolysis of $(\text{Phebox})\text{Ir}(\text{OAc})_2(\text{OH}_2)$ in C_6D_6 at 60 °C required almost 1 week to reach the same 98% conversion to $(\text{Phebox})\text{Ir}(\text{Phenyl-}d_5)(\text{OAc})$ (Figure 2). The data for the

Kinetics of Benzene Activation at 60 °C

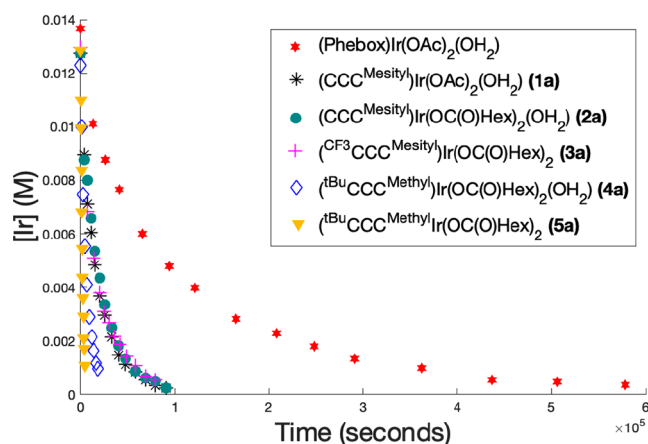


Figure 2. Reaction profiles for thermolysis of Ir carboxylate in C_6D_6 at 60 °C.

disappearance of the starting Ir complexes with respect to time fit exponential decays indicative of reaction rates that are first order in Ir-carboxylate (see Figures S1–S6).

As seen in Table 1, entries 1 and 2, the reaction of **1a** with C_6D_6 at 60 °C to form its Ir-phenyl product proceeds 6 times faster than that of $(\text{Phebox})\text{Ir}(\text{OAc})_2(\text{OH}_2)$.

The reaction of the hexanoate derivative **2a** with C_6D_6 at 60 °C proceeded to form $(\text{CCC}^{\text{Mesityl}})\text{Ir}(\text{Phenyl-}d_5)(\text{OC}(\text{O})\text{Hex})$ (**2b**) with a k_{obs} value similar to that of the acetate complex **1a** (Table 1). This result is consistent with observations made

Table 1. Observed C₆D₆ Activation Rates at 60 °C

	complex	k_{obs} at 60 °C (s ⁻¹)
1	(Phebox)Ir(OAc) ₂ (OH ₂)	$(9.1 \pm 0.1) \times 10^{-6}$
2	1a	$(5.8 \pm 0.1) \times 10^{-5}$
3	2a	$(4.6 \pm 0.3) \times 10^{-5}$
4	3a	$(4.7 \pm 0.5) \times 10^{-5}$
5	4a	$(1.5 \pm 0.1) \times 10^{-4}$
6	5a	$(5.4 \pm 0.1) \times 10^{-4}$

by Yuan et al. that variations in the carboxylate groups had essentially no effect on *n*-octane activation by (Phebox)Ir(OC(O)R)₂(H₂O) complexes.¹⁸

On the basis of the computational results previously reported,¹⁹ we postulated that a more electrophilic metal center might promote a higher rate of C–H bond activation. To probe this hypothesis, (CF₃CCC^{Mesityl})Ir(OC(O)Hex)₂ (**3a**) was synthesized (Scheme 1). Of note, complex **3a** did not crystallize with a bound H₂O. Instead, one acetate ligand binds in a κ² fashion (Figure S12, ORTEP diagram of **3a**). Interestingly, the rate of reaction of **3a** with benzene at 60 °C to form (CF₃CCC^{Mesityl})Ir(Phenyl-*d*₅)(OC(O)Hex) (**3b**) was virtually identical with that of **2a** to form its phenyl derivative (Table 1).

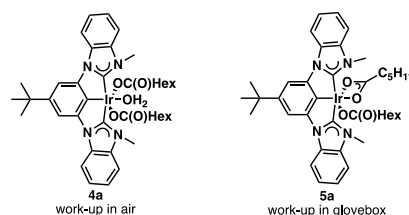
The C–D bond activation reactions of all the complexes were studied at varied temperatures from 60 to 100 °C, and the activation parameters for the reactions were calculated from the rate data (Table 2). The faster rate observed for the reaction of **1a** versus that of the Phebox derivative is due to a lower Δ*H*[‡] value (22.7 ± 0.3 kcal/mol versus 26 ± 1 kcal/mol, respectively). In contrast, the Δ*S*[‡] value for the reaction of the (Phebox)Ir(OAc)₂(OH₂) complex is ~6 eu more favorable than that of **1a**. The Δ*G*[‡] value calculated at 60 °C shows that the reaction of **1a** experiences a reaction barrier that is about 1 kcal/mol lower than that of (Phebox)Ir(OAc)₂(OH₂) (Table 2).

The Δ*H*[‡] and Δ*G*[‡] values calculated for the reaction of the hexanoate derivative **2a** with C₆D₆ are the same within error as those found for acetate complex **1a**, providing further evidence that the nature of the carboxylate has little effect on the C–H activation barrier in CMD reactions of Ir^{III}.¹⁸ The Δ*S*[‡] value is slightly more negative for **2a**, likely due to increased sterics of the hexanoate in comparison to the acetate ligand.

The more negative Δ*S*[‡] values determined for C–D activation by **1a** and **2a** in comparison to that of (Phebox)Ir(OAc)₂(OH₂) imply that greater order is required in the transition states for **1a** and **2a**. It was considered that the steric bulk of the flanking mesityl groups bound to the CCC ligand (Figure 1) could limit the approach of the benzene, constraining it to the plane perpendicular to the central phenyl and benzimidazole rings of the CCC ligand.²¹ Thus, decreasing the sterics near the metal center might allow for a less ordered

transition state. An analogous CCC ligand with methyl groups on the carbene ligand in place of mesityl rings is known.²² To increase the solubility and also the selectivity for tridentate coordination of the CCC^{Methyl} ligand when it is metalated to Ir,²³ a *tert*-butyl group was appended to the *para* position of the central arene ring, making the ligand denoted as ^{*t*Bu}CCC^{Methyl}.

The Ir complex (^{*t*Bu}CCC^{Methyl})Ir(OC(O)Hex)₂(OH₂) (**4a**; Figure 3) was synthesized and fully characterized. Thermolysis

**Figure 3.** Water-ligated and anhydrous ^{*t*Bu}CCC^{Methyl} complexes. See Figure S15 for an ORTEP diagram of **4a**.

of **4a** in C₆D₆ led to the expected phenyl product, (^{*t*Bu}CCC^{Methyl})Ir(Phenyl-*d*₅)(OC(O)Hex) (**4b**) (Figure S16, ORTEP diagram of **4b**). The rate of benzene activation at 60 °C by **4a** was 3 times faster than the analogous reaction of **2a** (Table 1, entries 5 and 3). The greater k_{obs} value is consistent with the hypothesis that reduced sterics near the metal center would increase the rate of benzene activation. Further, it was demonstrated that a larger Δ*S*[‡] value was responsible for the increase in rate (Table 2, entry 4). Yet, the replacement of the flanking mesityls with methyl groups resulted in a significant increase in the Δ*H*[‡] value, and overall, the Δ*G*[‡] value for the reaction of **4a** was lowered by only ca. 1 kcal/mol in comparison to that of **2a**.

The thermolysis reactions represented in Tables 1 and 2 were carried out in C₆D₆ that was dried over Na⁰/benzophenone. In experiments carried out with untreated commercial samples of C₆D₆ (Table S18), significantly slower rates of C–D activation were observed. We hypothesized that the water present in the untreated benzene solvent inhibited the C–D activation reactions. This hypothesis is consistent with the mechanism proposed in computational studies of C–H activation by (Phebox)Ir(OAc)₂H₂O,¹⁹ where the aquo ligand dissociates prior to C–D activation.

To investigate this proposal of preliminary water loss from **4a**, (^{*t*Bu}CCC^{Methyl})Ir(OC(O)Hex)₂ (**5a**), which bears a κ²-OC(O)Hex group and no water ligand, was synthesized and purified under a dry nitrogen atmosphere (Figure 3, right). The broad singlet at 10.3 ppm attributed to the ligated water protons (hydrogen bonding to the hexanoate groups) observed in ¹H NMR spectra of **4a** (C₆D₆) is absent in the spectrum of **5a** (Figure S17). In addition, the ¹H NMR multiplets

Table 2. Eyring Analysis of C₆D₆ Activation

	complex	Δ <i>H</i> [‡] (kcal/mol)	Δ <i>S</i> [‡] (cal/(mol K))	Δ <i>G</i> [‡] (kcal/mol) ^a
1	(Phebox)Ir(OAc) ₂ (OH ₂)	26 ± 1	−4 ± 1	27.3 ± 0.3
2	1a	22.7 ± 0.3	−10 ± 1	26.0 ± 0.6
3	2a	22.3 ± 0.7	−12 ± 1	26.2 ± 1.7
4	4a	27.2 ± 0.8	5 ± 1	25.4 ± 1.6
5	5a	19.0 ± 0.5	−17 ± 1	24.6 ± 0.6

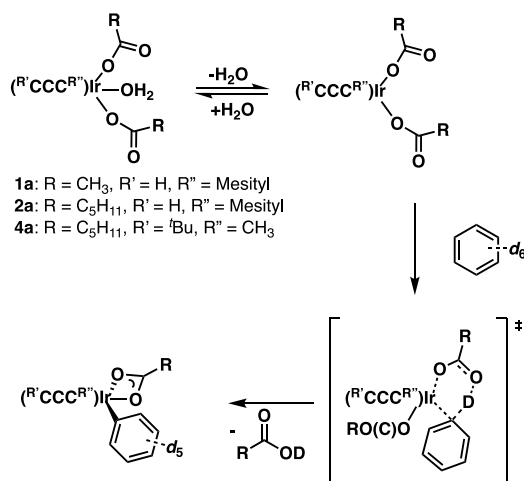
^aΔ*G*[‡] calculated for reaction at 60 °C.

corresponding to the protons on the hexanoate ligands in **5a** are shifted downfield relative to the signals attributed to the same protons of **4a**. Titration of 1 equiv of water into a sample of **5a** resulted in a ^1H NMR spectrum which matched that of **4a** (Figure S18).

Thermolysis of **5a** in dry C_6D_6 led to the expected product, **4b**, and the rate of benzene activation at 60°C by **5a** was 3 times faster than the analogous reaction of **4a**. This experiment clearly demonstrates the inhibitory effect of water on the reaction. The greater facility of **5a** in promoting C–D activation of C_6D_6 makes it such that the reaction can be observed at temperatures as low as 30°C , reaching a 90% yield after 22 h.

Comparing the activation parameters determined for the reaction of **5a** with those of **4a** provides insight into the effect of the aquo ligand on the C–D activation reaction. The ΔH^\ddagger value for the reaction of **5a** with C_6D_6 (19.0 ± 0.5 kcal/mol) is 8 kcal/mol lower than that of **4a**. Moreover, the ΔS^\ddagger value for the reaction of **5a** is 22 eu more negative than for **4a**. The decreases in ΔH^\ddagger and ΔS^\ddagger values are consistent with the mechanistic proposal shown in Scheme 3 for the (CCC)Ir–

Scheme 3. Proposed Mechanism of H_2O Dissociation followed by CMD of Benzene to Make Ir-Phenyl Complexes



(OC(O)R)₂(H₂O) complexes. Initial dissociation of the water yields an intermediate with κ^1 -carboxylates and an open site on the Ir. The benzene can then approach the open site and undergo CMD with a carboxylate. Without an aquo ligand, **5a** only has to open one carboxylate from κ^2 to κ^1 to allow for a similar CMD reaction with benzene rather than fully dissociate a ligand. The rapid uptake of water to generate **4a** from **5a** is consistent with the facility of the carboxylate opening and also with the strong preference of these complexes to bind water. The contrast in the ΔS^\ddagger values for **5a** and **4a** is striking, but the negative ΔS^\ddagger value observed for the reaction of **5a** is rationalized by the absence of the very positive contribution to ΔS^\ddagger resulting from the water ligand dissociation from **4a**.

Notably, the reaction of the ($\text{CF}_3\text{CCC}^{\text{Mesityl}}$) complex **3a**, which lacks an aquo ligand, proceeded at a rate similar to that for the $\text{CCC}^{\text{Mesityl}}$ complex **2a**, under both wet and dry conditions (Table 1 and Table S18). This similarity in rate between **3a** and **2a** suggests that the electron-withdrawing substituent actually disfavors the C–D activation reaction. If the CF_3 did not affect the benzene activation, the rate

exhibited by **3a**, which lacks an aquo ligand, would be expected to be greater than that of **2a**.

CONCLUSION

In summary, by replacement of the oxazoline rings of the first generation Phebox system, (Phebox)Ir(OAc)₂(OH₂), with carbene moieties, lowering of the steric bulk around the metal center, and elimination of the aquo ligand, the rate of C–D activation of benzene increased by 2 orders of magnitude (Table 1, entries 1 and 6). Overall, the ΔG^\ddagger value for benzene activation at 60°C by **5a** is ca. 3 kcal/mol lower than that of the first-generation carboxylate complex, (Phebox)Ir(OAc)₂(OH₂). Our results using kinetic studies to inform ligand design are also promising for the development of effective catalysts for aerobic transformations of alkanes. While initial investigations of the reactivity of **5a** in *n*-octane were compromised by extremely low solubility, using the design principles as outlined above, further modifications of our ligand are underway.

EXPERIMENTAL SECTION

General Information. Unless otherwise specified, all reactions were carried out under an inert nitrogen atmosphere using either Schlenk techniques or a glovebox. Toluene, methylene chloride, and acetonitrile were dried by passage through activated alumina and molecular sieve columns under a stream of argon gas (a Grubbs type solvent purification system by JC Meyer Solvent Systems). 2-Ethoxyethanol and DMSO were dried over 3 Å sieves and sparged with N₂. Octane, 98%+, was purchased from Alfa Aesar, stirred with H₂SO₄, distilled, sparged with N₂, and dried over 3 Å sieves. All deuterated solvents were purchased from Cambridge Isotope Laboratories. For the purposes of characterization of (CCC)Ir complexes, CDCl₃ and CD₂Cl₂ were used as received. C_6D_6 was dried over sodium/benzophenone and stored in the glovebox. All other solvents were used as received. ^1H and $^{13}\text{C}\{^1\text{H}\}$ NMR spectra were recorded on Bruker NEO 600 MHz equipped with a Prodigy probe, Avance III 500 MHz, and Avance II 400 MHz spectrometers and referenced to the residual solvent peak. All NMR spectra were recorded at ambient probe temperatures. All chemical shifts (δ) are reported in ppm. ^{19}F NMR shifts are reported relative to a monofluorobenzene standard. ($^{\text{dm}}\text{Phebox}$)Ir(OAc)₂(OH₂) was prepared according to literature procedures,⁹ as were ($^{\text{RCCC}^{\text{Mesityl}}}\text{Ir}(\text{H})(\text{Cl})(\text{CH}_2\text{Cl}_2)$)²⁰ and [$\mu\text{-O}(\text{Me})\text{COD}$]₂.²⁴ Detailed procedures for the preparation of ($^{\text{RCCC}^{\text{Mesityl}}}\text{Ir}(\text{H})(\text{Cl})(\text{CH}_2\text{Cl}_2)$) are included in the Supporting Information. Elemental analyses were performed by Dr. William Brennessel at the University of Rochester. Accurate mass measurement analyses were conducted on a Waters LCT Premier XE time of flight LCMS instrument with electrospray ionization (ESI). The signals were mass-measured against an internal lock mass reference of leucine enkephalin. Crystal structure determination was done by Dr. Patrick Carroll and Dr. Michael Gau at the University of Pennsylvania.

($^{\text{RCCC}^{\text{Mesityl}}}\text{Ir}(\text{OC}(\text{O})\text{R}')_2 \cdot n\text{OH}_2$) (R = H, CF₃, R' = CH₃, C₆H₁₁). Described is the general method by which ($^{\text{RCCC}^{\text{Mesityl}}}\text{Ir}$) carboxylate complexes were synthesized. Approximately 0.5 mmol of ($^{\text{RCCC}^{\text{Mesityl}}}\text{Ir}(\text{H})(\text{Cl})(\text{CH}_2\text{Cl}_2)$) was combined with 6 equivalents of Ag(OC(O)R') in a 250 mL Schlenk flask under N₂. A 50 mL portion of dry methylene chloride was added, and the flask was wrapped in foil. The mixture was refluxed with stirring for 16 h under an N₂ atmosphere. After the reaction mixture was cooled, it was filtered through Celite and the filtrate was reduced to an oil. ($^{\text{RCCC}^{\text{Mesityl}}}\text{Ir}(\text{OC}(\text{O})\text{R}')_2 \cdot n\text{OH}_2$) was purified by flash chromatography on silica gel.

($^{\text{CCC}^{\text{Mesityl}}}\text{Ir}(\text{OAc})_2(\text{OH}_2)$) (**1a**). Complex **1a** was further purified by recrystallization from methylene chloride. Yield: 64%. ^1H NMR (600 MHz, CD₂Cl₂): δ 8.25 (d, *J* = 8.3 Hz, 2H), 7.73 (d, *J* = 7.9 Hz, 2H), 7.49 (t, *J* = 7.7 Hz, 2H), 7.35–7.29 (m, 3H), 7.08 (s, 4H), 7.00 (t, *J* =

8.0 Hz, 2H), 2.42 (s, 6H), 1.90 (s, 12H), 1.34 (s, 6H). $^{13}\text{C}\{^1\text{H}\}$ NMR (151 MHz, CD_2Cl_2): δ 184.64, 181.28, 148.58, 140.11, 137.49, 136.04, 135.69, 133.02, 132.52, 129.64, 124.58, 123.65, 123.03, 111.93, 111.75, 108.63, 22.31, 21.54, 17.44. Anal. Calcd for $\text{C}_{42}\text{H}_{41}\text{IrN}_4\text{O}_5$: C, 57.72; H, 4.73; N, 6.41. Found: C, 57.72; H 4.56; N, 6.29.

$(\text{CCC}^{\text{Mesityl}})\text{Ir}(\text{OC}(\text{O})\text{Hex})_2(\text{OH}_2)$ (**2a**). Complex **2a** was isolated as a yellow powder after chromatography by evaporation of the eluent *in vacuo*. Yield: 71%. ^1H NMR (500 MHz, CD_2Cl_2): δ 8.19 (d, $J = 8.2$ Hz, 2H), 7.66 (d, $J = 8.0$ Hz, 2H), 7.42 (t, 2H), 7.26 (t, $J = 7.6$ Hz, 2H), 7.21 (t, $J = 7.9$ Hz, 1H), 7.00 (s, 4H), 6.93 (d, $J = 8.0$ Hz, 2H), 2.34 (s, 6H), 1.86 (s, 12H), 1.55 (t, $J = 7.3$ Hz, 4H), 1.03 (dq, $J = 14.3$, 7.2 Hz, 4H), 0.86 (p, $J = 3.6$ Hz, 8H), 0.69 (t, $J = 7.4$ Hz, 6H). $^{13}\text{C}\{^1\text{H}\}$ NMR (126 MHz, CD_2Cl_2): δ 185.19, 184.76, 148.48, 139.97, 137.42, 136.10, 134.58, 133.00, 132.80, 129.68, 124.51, 123.61, 122.87, 111.91, 111.76, 108.37, 35.83, 31.97, 24.86, 22.98, 21.51, 17.80, 14.32. Anal. Calcd for $\text{C}_{50}\text{H}_{47}\text{IrN}_4\text{O}_5$: C, 60.89; H, 5.83; N, 5.68. Found: C, 61.229; H, 5.71; N, 5.202. See Figure S11 for the crystal structure.

$(\text{CF}_3\text{CCC}^{\text{Mesityl}})\text{Ir}(\text{OC}(\text{O})\text{Hex})_2$ (**3a**). Complex **3a** was isolated as a yellow powder after chromatography by evaporation of the eluent *in vacuo*. Yield: 75%. ^1H NMR (600 MHz, CD_2Cl_2): δ 8.28 (d, $J = 8.2$ Hz, 2H), 7.93 (s, 2H), 7.54 (t, $J = 7.7$ Hz, 2H), 7.37 (t, $J = 7.7$ Hz, 2H), 7.08 (s, 4H), 7.02 (d, $J = 8.0$ Hz, 2H), 2.41 (s, 6H), 1.91 (s, 12H), 1.63 (t, $J = 7.5$ Hz, 4H), 1.08 (q, $J = 7.2$ Hz, 4H), 0.92 (dq, $J = 11.2$, 6.4, 4.8 Hz, 9H), 0.73 (t, $J = 7.4$ Hz, 6H). $^{13}\text{C}\{^1\text{H}\}$ NMR (151 MHz, CD_2Cl_2): δ 184.58, 183.96, 148.31, 140.27, 137.37, 136.04, 132.72, 132.31, 129.76, 128.83 (q, $^1J_{\text{CF}} = 271.0$ Hz) 124.89, 124.79 (q, $^2J_{\text{CF}} = 31.2$ Hz), 124.68, 124.14, 111.99, 105.38, 105.35, 35.88, 31.95, 25.28, 22.88, 21.53, 17.69, 14.24. $^{19}\text{F}\{^1\text{H}\}$ NMR (376 MHz, CD_2Cl_2): δ -60.32. Anal. Calcd for $\text{C}_{51}\text{H}_{54}\text{F}_3\text{IrN}_4\text{O}_4$: C, 59.11; H, 5.25; N, 5.41. Found: C, 59.15; H, 5.19; N, 5.35. See Figure S12 for the crystal structure.

1,1'-(5-(tert-Butyl)-1,3-phenylene)bis(1-benzimidazole) (L6). This procedure was adapted from the literature preparation of a related complex.²² A Schlenk flask was charged with CuI (1 mmol), *N,N*-dimethylglycine (2.1 mmol), K_2CO_3 (20 mmol), 1,3-dibromo-5-(tert-butyl)benzene (4.93 mmol), and benzimidazole (12.5 mmol). The system was placed under an N_2 atmosphere, and 15 mL of dry, N_2 -sparged DMSO was added via cannula transfer. The mixture was heated in a 120 °C oil bath for 54 h. The crude product mixture was extracted into 20 mL of ethyl acetate and washed six times with 100 mL of water to remove DMSO. The organic layer was concentrated on the rotary evaporator and then purified by flash chromatography using a 30% mixture of ethyl acetate in hexanes followed by a gradient from 0 to 5% methanol in methylene chloride as eluents. The product was collected as a pink oil, after removal of the eluent by rotary evaporation, and was recrystallized from methylene chloride, giving a colorless crystalline product. Yield: 52%. ^1H NMR (600 MHz, CDCl_3): δ 8.19 (s, 2H), 7.94–7.89 (m, 2H), 7.64 (d, $J = 1.9$ Hz, 2H), 7.61–7.55 (m, 2H), 7.52 (t, $J = 1.9$ Hz, 1H), 7.38 (dt, $J = 7.2$, 1.9 Hz, 4H), 1.47 (s, 9H). $^{13}\text{C}\{^1\text{H}\}$ NMR (151 MHz, CDCl_3): δ 156.40, 144.32, 142.16, 137.86, 133.62, 124.26, 123.32, 121.10, 120.80, 116.65, 110.34, 35.63, 31.36. Accurate mass measurement (ESI+, TOF) m/z [$\text{M} + \text{H}^+$] $\text{C}_{24}\text{H}_{23}\text{N}_4$: theoretical mass, 367.1923; observed mass, 367.1920.

1,1'-(5-(tert-Butyl)-1,3-phenylene)bis(3-methyl-1-benzimidazole) iodide ($(^{\text{tBu}}\text{CCC}^{\text{Methyl}})\text{Ligand}$). This procedure was adapted from the literature.²² **L6** (0.85 mmol, 1 equiv), MeI (4.2 mmol, 5 equiv), and 10 mL of dry acetonitrile were dispensed into a 50 mL flask sealed with a Teflon stopcock. The mixture was placed under an N_2 atmosphere and heated to reflux overnight. The resulting suspension of a white solid in a yellow solution was evacuated to dryness on a Schlenk line. The white solid was suspended in pentane, collected on a frit, and dried *in vacuo*. Yield: 88%. ^1H NMR (600 MHz, $\text{DMSO}-d_6$): δ 9.49 (s, 2H), 7.48–7.30 (m, 5H), 7.21 (d, $J = 8.3$ Hz, 2H), 7.00 (t, $J = 7.8$ Hz, 2H), 6.95 (t, $J = 7.8$ Hz, 2H), 3.42 (s, 6H), 0.64 (s, 9H). $^{13}\text{C}\{^1\text{H}\}$ NMR (151 MHz, chloroform-*d*): δ 156.10, 143.55 (td, $^1J_{\text{CN}} = 11.85$, 6.05), 134.25, 131.83, 130.74, 127.56, 127.10, 124.20, 114.06, 113.52, 35.62, 33.66, 30.70. Accurate

mass measurement (ESI+, TOF) m/z [MI^+] $\text{C}_{26}\text{H}_{28}\text{N}_4$: theoretical mass, 523.1359; observed mass, 523.1371.

$(^{\text{tBu}}\text{CCC}^{\text{Methyl}})\text{Ir}(\text{I})_2$. In a glovebox under a N_2 atmosphere, the ligand $(^{\text{tBu}}\text{CCC}^{\text{Methyl}})$ (0.769 mmol, 1 equiv) and KI (4.7 mmol, 6 equiv) were dispensed into a 50 mL Schlenk flask, along with 5 mL of dry, N_2 -sparged 2-ethoxyethanol. The flask was removed from the glovebox and equipped with an N_2 -flushed addition funnel. In the N_2 glovebox, $[\text{Ir}(\mu\text{-OMe})\text{COD}]_2$ (0.4 mmol, 0.5 equiv) was dispensed into a 50 mL vessel equipped with a Teflon pin and dissolved in 10 mL of dry, N_2 -sparged 2-ethoxyethanol. The $[\text{Ir}(\mu\text{-OMe})\text{COD}]_2$ solution was then removed from the glovebox, gently heated until homogeneous, cooled, and transferred via cannula to the N_2 -flushed addition funnel attached to the Schlenk flask containing the ligand and KI. The Schlenk flask was heated to 120 °C, and the $[\text{Ir}(\mu\text{-OMe})\text{COD}]_2$ solution was added dropwise. The addition funnel was replaced with an N_2 -flushed reflux condenser, and the mixture was heated to reflux for 20 h, forming a yellow solution with a dark orange solid. The solid was isolated by cannula filtration, rinsed with 2-ethoxyethanol, and then dried under high vacuum. Yield: 80%. ^1H NMR (600 MHz, CDCl_3): δ 8.16 (d, $J = 8.0$ Hz, 2H), 7.72 (s, 2H), 7.48 (t, $J = 7.6$ Hz, 2H), 7.43 (t, $J = 7.4$ Hz, 2H), 7.38 (d, $J = 7.9$, 2H), 4.12 (s, 6H), 1.52 (s, 9H). $^{13}\text{C}\{^1\text{H}\}$ NMR (151 MHz, CDCl_3): δ 176.47, 147.47, 145.09, 136.11, 132.69, 131.86, 123.90, 123.02, 111.54, 110.48, 106.53, 35.62, 35.15, 32.37. Accurate mass measurement (ESI+, TOF) m/z [$\text{M} + \text{H}^+$] $\text{C}_{52}\text{H}_{51}\text{I}_2\text{Ir}_2\text{N}_8$: theoretical mass, 1678.9653; observed mass, 1678.9639. See Figure S14 for the crystal structure.

$(^{\text{tBu}}\text{CCC}^{\text{Methyl}})\text{Ir}(\text{OC}(\text{O})\text{Hex})_2 \cdot n\text{OH}_2$. This reaction was set up in a glovebox under an N_2 atmosphere. $[(^{\text{tBu}}\text{CCC}^{\text{Methyl}})\text{Ir}(\text{I})_2]$ (0.12 mmol, 0.5 equiv) and $\text{AgOC}(\text{O})\text{Hex}$ (1.4 mmol, 6 equiv) were dispensed into a 100 mL Schlenk flask equipped with a stir bar. A 28 mL portion of chloroform (dried over CaH_2 , distilled, and sparged with N_2) was added. The flask was wrapped in aluminum foil and equipped with an N_2 -flushed reflux condenser. The mixture was refluxed for 4.5 h and then brought into the glovebox and filtered through a PTFE syringe filter. The yellow filtrate was evacuated to form a yellow-brown oil. The oil was dissolved in 5 mL of THF, reduced to 0.5 mL, and then 10 mL of pentane was added. A pale yellow solid crashed out, was isolated on a frit, and rinsed with diethyl ether. The yellow solid was $(^{\text{tBu}}\text{CCC}^{\text{Methyl}})\text{Ir}(\text{OC}(\text{O})\text{Hex})_2$ (**5a**) and was isolated in 59% yield.

Recrystallization of **5a** on the benchtop by slow evaporation of methylene chloride resulted in coordination of an aquo ligand to give $(^{\text{tBu}}\text{CCC}^{\text{Methyl}})\text{Ir}(\text{OC}(\text{O})\text{Hex})_2(\text{OH}_2)$ (**4a**), which was isolated in 55% yield. **4a** and **5a** are indistinguishable by ^1H NMR in CD_2Cl_2 and CDCl_3 but have different spectra in C_6D_6 (see Figures S17 and S18). ^1H NMR (600 MHz, CD_2Cl_2): δ 8.17 (d, $J = 8.3$ Hz, 2H), 7.73 (s, 2H), 7.60 (d, $J = 8.3$ Hz, 2H), 7.49 (t, $J = 7.9$ Hz, 2H), 7.45 (t, $J = 7.6$ Hz, 2H), 4.49 (s, 6H), 1.71 (t, $J = 7.2$ Hz, 4H), 1.62 (s, 9H), 1.12 (p, $J = 7.3$ Hz, 4H), 0.96–0.88 (m, 4H), 0.82–0.74 (m, 4H), 0.56 (t, $J = 7.4$ Hz, 6H). $^{13}\text{C}\{^1\text{H}\}$ NMR (151 MHz, CDCl_3): δ 186.46, 186.23, 147.41, 147.26, 135.92, 133.08, 125.61, 123.83, 122.77, 111.27, 111.06, 106.08, 35.65, 35.23, 33.89, 32.53, 31.55, 25.66, 22.50, 22.44, 14.07. Anal. Calcd for $\text{C}_{38}\text{H}_{49}\text{IrN}_4\text{O}_5$ (aquo species **4a**): C, 54.72; H, 5.92; N, 6.72. Found: C, 54.38; H, 5.75; N, 6.51. See Figure S15 for the crystal structure of **4a**.

$(\text{R}'\text{CCC}^{\text{R}''})\text{Ir}(\text{C}_6\text{D}_5)(\text{OC}(\text{O})\text{R})$. This reaction was set up in a glovebox under an N_2 atmosphere. A 0.01 mmol sample of $(\text{R}'\text{CCC}^{\text{R}''})\text{Ir}(\text{OC}(\text{O})\text{R}')_2 \cdot n\text{OH}_2$ was dispensed into an NMR tube with a J. Young style cap. A 0.4 mL portion of benzene-*d*₆ was added, giving a homogeneous yellow solution. The NMR tube was sealed and placed in a 100 °C oil bath for 1.5 h. The NMR tube was cooled, and then the benzene-*d*₆ was removed by lyophilization on a Schlenk line. The resulting yellow solid was recrystallized and isolated.

$(\text{CCC}^{\text{Mesityl}})\text{Ir}(\text{C}_6\text{D}_5)(\text{OAc})$ (**1b**; $\text{R}' = \text{H}$, $\text{R} = \text{CH}_3$, $\text{R}'' = \text{Mesityl}$). Yield: 81%. ^1H NMR (500 MHz, C_6D_6): δ 7.79 (d, $J = 8.2$ Hz, 2H), 7.63 (d, $J = 7.9$ Hz, 2H), 7.40 (t, $J = 7.9$ Hz, 1H), 7.03 (t, $J = 7.7$ Hz, 2H), 6.87 (t, $J = 7.6$ Hz, 2H), 6.74 (s, 4H), 6.58 (d, $J = 8.0$ Hz, 2H), 2.02 (s, 6H), 1.99 (s, 6H), 1.61 (s, 3H), 1.47 (s, 6H). $^{13}\text{C}\{^1\text{H}\}$ NMR (126 MHz, C_6D_6): δ 188.89, 183.52, 147.16, 146.58, 138.87, 137.60,

136.81, 136.28, 133.24, 132.89, 132.80, 129.90, 128.99, 125.67, 123.59, 123.08, 120.74, 111.58, 110.89, 108.82, 25.21, 21.07, 17.63, 17.61. The triplet corresponding to the carbon para to Ir on the phenyl ring was not resolved, likely obscured by the solvent residual peak. Anal. Calcd for $C_{46}H_{33}D_3IrN_4O_2$: C, 62.85; H, 4.70; N, 6.37. Found: C, 63.42; H, 4.75; N, 6.19.

($CCC^{Mesityl}$)Ir(C_6D_5)(OC(O)Hex) (**2b**; $R' = H$, $R = C_5H_{11}$, $R'' = Mesityl$). Yield: 71%. 1H NMR (500 MHz, C_6D_6): δ 7.80 (d, $J = 8.2$ Hz, 2H), 7.65 (d, $J = 7.9$ Hz, 2H), 7.41 (t, $J = 7.8$ Hz, 1H), 7.04 (t, $J = 7.8$, 2H), 6.87 (t, $J = 7.6$ Hz, 2H), 6.83 (s, 2H), 6.78 (s, 2H), 6.57 (d, $J = 8.0$ Hz, 2H), 2.15 (s, 6H), 2.05–1.99 (m, 3H), 1.96 (s, 6H), 1.50 (s, 6H), 1.44 (q, $J = 6.9$ Hz, 1H), 1.36–1.28 (m, 4H), 1.03 (t, $J = 7.3$ Hz, 3H). $^{13}C\{^1H\}$ NMR (126 MHz, C_6D_6): δ 188.84, 185.69, 147.22, 146.55, 138.71, 137.67, 136.78, 136.27, 133.20 (t), 133.07, 132.78, 129.79, 129.12, 127.52, 125.70 (t), 123.62, 123.08, 120.84, 120.74, 111.56, 110.89, 108.80, 38.62, 32.55, 24.13, 23.46, 21.16, 17.75, 17.67, 14.71. The triplet corresponding to the carbon para to Ir on the phenyl ring was not resolved, likely obscured by the solvent residual peak. Anal. Calcd for $C_{50}H_{44}D_3IrN_4O_2$: C, 64.02; H, 5.28; N, 5.99. Found: C, 64.15; H, 5.34; N, 5.82. See figure S13 for crystal structure.

($CF_3CCC^{Mesityl}$)Ir(C_6D_5)(OC(O)Hex) (**3b**; $R' = CF_3$, $R = C_5H_{11}$, $R'' = Mesityl$). Yield: 90%. 1H NMR (500 MHz, C_6D_6): δ 8.02 (s, 2H), 7.69 (d, $J = 8.2$ Hz, 2H), 6.93 (t, $J = 7.7$ Hz, 2H), 6.84 (t, $J = 7.8$ Hz, 2H), 6.82 (d, $J = 2.4$ Hz, 2H), 6.78 (s, 2H), 6.52 (d, $J = 7.9$ Hz, 2H), 2.15 (s, 6H), 2.04–1.99 (m, 1H), 1.97 (s, 6H), 1.46 (s, 6H), 1.43 (d, $J = 10.2$ Hz, 3H), 1.31 (h, $J = 3.9$ Hz, 4H), 1.03 (t, $J = 7.3$ Hz, 3H). $^{13}C\{^1H\}$ NMR (126 MHz, C_6D_6): δ 188.50, 186.17, 155.16, 146.35, 138.95, 137.57, 136.57, 136.09, 132.96, 132.80 (t, $J = 18.9$ Hz), 132.79, 132.37, 129.87, 129.18, 125.91 (t, $J = 22.6$ Hz), 126.65 (q, $J = 218.2$ Hz), 124.12, 123.50, 122.615 (q, $J = 34.8$ Hz), 121.29 (t, $J = 21.02$), 120.21, 111.64, 110.92, 105.61, 38.60, 32.49, 24.01, 23.44, 21.15, 17.66, 17.54, 14.69. ^{19}F NMR (376 MHz, $C_6D_6F\{^1H\}$ NMR (376 MHz, C_6D_6): δ -59.20. Anal. Calcd for $C_{51}H_{43}D_3F_3IrN_4O_2$: C, 61.06; H, 4.82; N, 5.58. Found: C, 60.76; H, 4.70; N, 5.46.

($^tBuCCC^{Methyl}$)Ir(C_6D_5)(OC(O)Hex) (**4b**; $R' = ^tBu$, $R = C_5H_{11}$, $R'' = Methyl$). Yield: 90%. 1H NMR (400 MHz, THF- d_8): δ 8.20 (d, $J = 8.1$ Hz, 2H), 7.75 (s, 2H), 7.53 (d, $J = 7.5$ Hz, 2H), 7.41 (t, $J = 7.7$ Hz, 1H), 7.32 (t, $J = 7.5$ Hz, 2H), 4.21 (s, 6H), 2.25 (t, $J = 7.5$ Hz, 2H), 1.71–1.67 (m, 2H; multiplet at 1.71–1.67 ppm partially obscured by the solvent residual peak), 1.62 (s, 9H), 1.34 (m, 4H), 0.88 (t, $J = 7.0$ Hz, 3H). $^{13}C\{^1H\}$ NMR (126 MHz, THF- d_8): δ 191.60, 187.47, 146.97, 145.49, 140.87, 137.12, 133.72 (t, $J = 22.6$ Hz), 133.67, 125.72 (t, $J = 23.2$ Hz), 124.21, 123.35, 122.38, 120.55 (t, $J = 23.2$ Hz), 111.85, 111.73, 106.50, 38.96, 36.23, 33.16, 32.95, 32.72, 14.55. Anal. Calcd for $C_{38}H_{36}D_3IrN_4O_2$: C, 58.29; H, 5.28; N, 7.16. Found: C, 58.08; H, 5.17; N, 6.92. See Figure S16 for the crystal structure.

($CCC^{Mesityl}$)Ir(Octyl)(OAc). In a N_2 -filled glovebox, *n*-octane (50 mL) and ($CCC^{Mesityl}$)Ir(OAc) $_2$ (OH) $_2$ (11 mg, 0.013 mmol) were combined in a 100 mL Schlenk flask with a Teflon stopper and stir bar. The mixture was heated to 105 °C for 24 h, giving a homogeneous yellow solution. The mixture was cooled, and all of the volatiles were removed under vacuum. A 50 mL portion of *n*-octane was added to the residue in the glovebox, and the mixture was heated for another 24 h at 105 °C. The solvent was removed from the dark yellow solution *in vacuo*, resulting in a yellow residue. In the N_2 -filled glovebox, the residue was dissolved in *n*-pentane and filtered through a PTFE syringe filter. The filtrate was loaded on a 1 in. silica plug, rinsed with 20 mL of pentane and then eluted with an 80/20 toluene/acetone mixture. The product was collected as an orange fraction, dried *in vacuo*, triturated with pentane, dried again, and then lyophilized from benzene. Isolated yield: 55%. 1H NMR (500 MHz, C_6D_6): δ 7.91 (d, 8.2 Hz, 2H), 7.67 (d, 7.9 Hz, 2H), 7.35 (t, 7.8 Hz, 1H), 7.10 (t, 8.0 Hz, 2H), 6.95 (t, 7.6 Hz, 2H), 6.84 (s, 2H), 6.75 (s, 2H), 6.71 (d, 8.4 Hz, 2H), 2.13 (s, 6H), 2.09 (s, 6H), 1.96 (s, 6H), 1.32 (s, 3H), 1.16–1.12 (m, 2H), 1.07 (bs, 6H), 1.01–0.98 (m, 4H), 0.94–0.89 (m, 2H), 0.79 (t, 7.1 Hz, 3H). $^{13}C\{^1H\}$ NMR (126 MHz, C_6D_6): δ 190.95, 183.38, 147.38, 146.31, 138.53, 137.39, 136.89, 136.74, 133.29, 132.98, 129.76, 129.47, 128.35, 123.48, 123.05, 119.37, 111.43, 110.75, 108.24, 32.23, 32.19, 31.63, 29.99, 29.95, 25.05, 23.05, 21.03, 18.00, 17.70, 14.34, -8.34 (Ir- C_{octyl}). Accurate

mass measurement (ESI+, TOF) m/z [$M + Na^+$] $C_{48}H_{53}IrN_4O_2Na$: theoretical mass, 933.3710; observed mass, 933.3699.

An analogous reaction was performed to make ($CF_3CCC^{Mesityl}$)Ir(Octyl)(OAc), which was isolated as single crystals, suitable for X-ray diffraction by slow evaporation of pentane in an N_2 glovebox (see Figure S10 for the crystal structure).

General Procedure for Kinetics Experiments. A 0.012 M stock solution of trimethoxybenzene in benzene- d_6 was prepared and dispensed into glass capillary tubes, which were then flame-sealed. In an N_2 -filled glovebox, between 2.5 and 4.5 mg of [Ir] was weighed out into an NMR tube equipped with a J. Young style Teflon cap. Each NMR tube was equipped with one trimethoxybenzene capillary. Then, 350 μ L of dry benzene- d_6 was placed in the tube. The initial 1H NMR spectrum was taken immediately, and then the sample was subsequently heated in an oil bath at a known temperature for consistent time intervals. e Spectra were taken at a minimum of 9 time points and data were recorded until the C–D activation reaction reached at least 87.5% conversion. Each time the sample was removed from the oil bath for analysis, it was first frozen in a dry ice/acetone bath to halt the reaction and then thawed to room temperature to take the 1H NMR spectrum. The disappearance of the [Ir] starting material was tracked relative to the trimethoxybenzene internal standard, plotted in MATLAB, and fit to a first-order exponential to find the k_{obs} value. See Figures S1–S6 for plots showing first-order decay fits to exponential functions.²⁵

■ ASSOCIATED CONTENT

Supporting Information

The Supporting Information is available free of charge at <https://pubs.acs.org/doi/10.1021/acs.organomet.1c00080>.

Synthetic details, NMR spectra, X-ray crystal structure information, and experimental details of the kinetic study (PDF)

Accession Codes

CCDC 2047612–2047620 contain the supplementary crystallographic data for this paper. These data can be obtained free of charge via www.ccdc.cam.ac.uk/data_request/cif, or by emailing data_request@ccdc.cam.ac.uk, or by contacting The Cambridge Crystallographic Data Centre, 12 Union Road, Cambridge CB2 1EZ, UK; fax: +44 1223 336033.

■ AUTHOR INFORMATION

Corresponding Author

Karen I. Goldberg – Department of Chemistry, University of Pennsylvania, Philadelphia, Pennsylvania 19104, United States; orcid.org/0000-0002-0124-1709; Email: kig@sas.upenn.edu

Authors

Sophie B. Rubashkin – Department of Chemistry, University of Pennsylvania, Philadelphia, Pennsylvania 19104, United States; orcid.org/0000-0002-9479-4109

Wan-Yi Chu – Department of Chemistry, University of Pennsylvania, Philadelphia, Pennsylvania 19104, United States; orcid.org/0000-0002-2599-9848

Complete contact information is available at:

<https://pubs.acs.org/doi/10.1021/acs.organomet.1c00080>

Notes

The authors declare no competing financial interest.

■ ACKNOWLEDGMENTS

This work was supported by the National Science Foundation (CHE-1856547), the CCI Center for Enabling New

Technologies through Catalysis (CENTC) (CHE-1205189), and the University of Pennsylvania. We thank the Vagelos Institute of Energy Science and Technology for a graduate fellowship to S.B.R. Accurate mass measurement was carried out by Dr. Charles W. Ross III (University of Pennsylvania), X-ray crystallography was carried out by Dr. Patrick Carroll and Dr. Michael Gau (University of Pennsylvania), and elemental analysis was carried out by Dr. William Brennessel (University of Rochester). The NSF Major Research Instrumentation Program (NSF CHE-1827457), the NIH Supplemental awards 3R01GM118510-03S1 and 3R01GM087605-06S1, and The Vagelos Institute for Energy Science and Technology are recognized for their support of NMR instrumentation used in this study. We thank Dr. Louise Guard and Dr. Ashley Wright for helpful discussions and guidance.

REFERENCES

- Arndtsen, B. A.; Bergman, R. G.; Mobley, T. A.; Peterson, T. H. Selective Intermolecular Carbon-Hydrogen Bond Activation by Synthetic Metal Complexes in Homogeneous Solution. *Acc. Chem. Res.* **1995**, *28*, 154–162.
- Goldberg, K. I.; Goldman, A. S. Large-Scale Selective Functionalization of Alkanes. *Acc. Chem. Res.* **2017**, *50*, 620–626.
- Choi, J.; MacArthur, A. H. R.; Brookhart, M.; Goldman, A. S. Dehydrogenation and Related Reactions Catalyzed by Iridium Pincer Complexes. *Chem. Rev.* **2011**, *111*, 1761–1779.
- Kumar, A.; Bhatti, T. M.; Goldman, A. S. Dehydrogenation of Alkanes and Aliphatic Groups by Pincer-Ligated Metal Complexes. *Chem. Rev.* **2017**, *117*, 12357–12384.
- Williams, D. B.; Kaminsky, W.; Mayer, J. M.; Goldberg, K. I. Reactions of iridium hydride pincer complexes with dioxygen: new dioxygen complexes and reversible O₂ binding. *Chem. Commun.* **2008**, 4195–4197.
- Morales-Morales, D.; Lee, D. W.; Wang, Z.; Jensen, C. M. Oxidative Addition of Water by an Iridium PCP Pincer Complex: Catalytic Dehydrogenation of Alkanes by IrH(OH){C₆H₃-2,6-(CH₂PBu^t)₂}. *Organometallics* **2001**, *20*, 1144–1147.
- Allen, K. E. *Synthesis of Electrophilic Rhodium and Iridium Complexes and Investigation of Reactivity for C-H Bond Activation and Functionalization*; Ph.D. Dissertation, Seattle, Washington, University of Washington, 2013.
- Ito, J.-i.; Kaneda, T.; Nishiyama, H. Intermolecular C–H Bond Activation of Alkanes and Arenes by NCN Pincer Iridium(III) Acetate Complexes Containing Bis(oxazolanyl)phenyl Ligands. *Organometallics* **2012**, *31*, 4442–4449.
- Allen, K. E.; Heinekey, D. M.; Goldman, A. S.; Goldberg, K. I. Alkane Dehydrogenation by C–H Activation at Iridium(III). *Organometallics* **2013**, *32*, 1579–1582.
- Frasco, D. A.; Mukherjee, S.; Sommer, R. D.; Perry, C. M.; Lambic, N. S.; Abboud, K. A.; Jakubikova, E.; Ison, E. A. Nondirected C–H Activation of Arenes with Cp*Ir(III) Acetate Complexes: An Experimental and Computational Study. *Organometallics* **2016**, *35*, 2435–2445.
- Walsh, A. P.; Jones, W. D. Mechanistic Insights of a Concerted Metalation–Deprotonation Reaction with [Cp*RhCl₂]₂. *Organometallics* **2015**, *34*, 3400–3407.
- Yang, L.; Zhang, Q.; Gao, J.; Wang, Y. Why Can Normal Palladium Catalysts Efficiently Mediate Aerobic C–H Hydroxylation of Arylpyridines by Intercepting Aldehyde Autoxidation? A Nascent Palladium(III)–Peracid Intermediate Makes a Difference. *Inorg. Chem.* **2019**, *58*, 4376–4384.
- Engle, K. M.; Wang, D.-H.; Yu, J.-Q. Ligand-Accelerated C–H Activation Reactions: Evidence for a Switch of Mechanism. *J. Am. Chem. Soc.* **2010**, *132*, 14137–14151.
- Jia, X.; Frye, L. I.; Zhu, W.; Gu, S.; Gunnoe, T. B. Synthesis of Stilbenes by Rhodium-Catalyzed Aerobic Alkenylation of Arenes via C–H Activation. *J. Am. Chem. Soc.* **2020**, *142*, 10534–10543.
- Gao, Y.; Guan, C.; Zhou, M.; Kumar, A.; Emge, T. J.; Wright, A. M.; Goldberg, K. I.; Krogh-Jespersen, K.; Goldman, A. S. β -Hydride Elimination and C–H Activation by an Iridium Acetate Complex, Catalyzed by Lewis Acids. Alkane Dehydrogenation Cocatalyzed by Lewis Acids and [2,6-Bis(4,4-dimethyloxazolanyl)-3,5-dimethylphenyl]iridium. *J. Am. Chem. Soc.* **2017**, *139*, 6338–6350.
- Wright, A. M.; Pahls, D. R.; Gary, J. B.; Warner, T.; Williams, J. Z.; Knapp, S. M. M.; Allen, K. E.; Landis, C. R.; Cundari, T. R.; Goldberg, K. I. Experimental and Computational Investigation of the Aerobic Oxidation of a Late Transition Metal-Hydride. *J. Am. Chem. Soc.* **2019**, *141*, 10830–10843.
- Allen, K. E.; Heinekey, D. M.; Goldman, A. S.; Goldberg, K. I. Regeneration of an Iridium(III) Complex Active for Alkane Dehydrogenation Using Molecular Oxygen. *Organometallics* **2014**, *33*, 1337–1340.
- Yuan, H.; Brennessel, W. W.; Jones, W. D. Effect of Carboxylate Ligands on Alkane Dehydrogenation with (^{dm}Phebox)Ir Complexes. *ACS Catal.* **2018**, *8*, 2326–2329.
- Pahls, D. R.; Allen, K. E.; Goldberg, K. I.; Cundari, T. R. Understanding the Effect of Ancillary Ligands on Concerted Metalation–Deprotonation by (^{dm}Phebox)Ir(OAc)₂(H₂O) Complexes: A DFT Study. *Organometallics* **2014**, *33*, 6413–6419.
- Chianese, A. R.; Drance, M. J.; Jensen, K. H.; McCollom, S. P.; Yusufova, N.; Shaner, S. E.; Shopov, D. Y.; Tendler, J. A. Acceptorless Alkane Dehydrogenation Catalyzed by Iridium CCC-Pincer Complexes. *Organometallics* **2014**, *33*, 457–464.
- Ghosh, R.; Emge, T. J.; Krogh-Jespersen, K.; Goldman, A. S. Combined Experimental and Computational Studies on Carbon–Carbon Reductive Elimination from Bis(hydrocarbyl) Complexes of (PCP)Ir. *J. Am. Chem. Soc.* **2008**, *130*, 11317–11327.
- Alabau, R. G.; Eguillor, B.; Esler, J.; Esteruelas, M. A.; Oliván, M.; Oñate, E.; Tsai, J.-Y.; Xia, C. CCC–Pincer–NHC Osmium Complexes: New Types of Blue-Green Emissive Neutral Compounds for Organic Light-Emitting Devices (OLEDs). *Organometallics* **2014**, *33*, 5582–5596.
- Raynal, M.; Pattacini, R.; Cazin, C. S. J.; Vallée, C.; Olivier-Bourbigou, H.; Braunstein, P. Reaction Intermediates in the Synthesis of New Hydrido, N-Heterocyclic Dicarbene Iridium(III) Pincer Complexes. *Organometallics* **2009**, *28*, 4028–4047.
- Pang, Y.; Ishiyama, T.; Kubota, K.; Ito, H. Iridium(I)-Catalyzed C–H Borylation in Air by Using Mechanochemistry. *Chem. - Eur. J.* **2019**, *25*, 4654–4659.
- Zhang, S.; Yang, S.; Lan, J.; Yang, S.; You, J. Helical nonracemic tubular coordination polymer gelators from simple achiral molecules. *Chem. Commun.* **2008**, 6170–6172.